Mechanical Writing of Ferroelectric Polarization

H. Lu *et al.*

Science **336**, 59 (2012);
DOI: 10.1126/science.1218693

Science (print ISSN 0036-8075; online ISSN 1095-9203) is published weekly, except the last week in December, by the American Association for the Advancement of Science, 1200 New York Avenue NW, Washington, DC 20005.

Mechanical Writing of Ferroelectric Polarization

H. Lu,[1] C.-W. Bark,[2] D. Esque de los Ojos,[3] J. Alcala,[4] C. B. Eom,[2] G. Catalan,[5,6]* A. Gruverman[1]*

Ferroelectric materials are characterized by a permanent electric dipole that can be reversed through the application of an external voltage, but a strong intrinsic coupling between polarization and deformation also causes all ferroelectrics to be piezoelectric, leading to applications in sensors and high-displacement actuators. A less explored property is flexoelectricity, the coupling between polarization and a strain gradient. We demonstrate that the stress gradient generated by the tip of an atomic force microscope can mechanically switch the polarization in the nanoscale volume of a ferroelectric film. Pure mechanical force can therefore be used as a dynamic tool for polarization control and may enable applications in which memory bits are written mechanically and read electrically.

Ferroelectrics strongly couple changes in polarization of a material with its deformation, which gives rise to useful electromechanical phenomena including piezoelectric, electrostrictive, and flexoelectric effects. Coupling between polarization and homogeneous in-plane strain can also be used to tune the symmetry and properties of ferroelectric thin films via strain engineering using different substrates (*1*, *2*). For a ferroelectric, however, the spontaneous strain (unit-cell deformation) is identical whether the polarization is pointing up or down, so one does not immediately think of mechanical deformation as a viable mechanism to invert the polarization in a ferroelectric memory.

Stress can nevertheless be used to influence polarization. A large local deformation can be realized by pressing the sharp tip of an atomic force microscope (AFM) against the surface of a film, thereby causing a large stress concentration near the tip-sample contact. Previous studies showed suppression of the piezoelectric response under a sufficiently high loading force (*3*, *4*), with almost complete recovery after stress release. Also, polarization vector rotation, caused by simultaneous application of an external electrical bias and tip-induced stress, has been observed in polycrystalline thin films (*4*, *5*), although in these studies the random orientation of the polarization in the crystals allowed for partial ferroelastic rotation rather than pure 180° inversion of polarization. The stress from adjacent grains also meant that the original polar configuration was recovered upon release of the tip pressure, so no permanent writing was achieved.

Recent reports by Lee *et al*. (*6*) show that the flexoelectric effect caused by strain gradients can create a strong imprint in uniaxial, perfectly oriented ferroelectric thin films, and flexoelectricity due to substrate bending was also invoked in the imprint of polarization in polycrystalline ferroelectric films (*7*). This suggests that strain gradients, rather than homogeneous strain, can be exploited for switching polarization and "writing" the domain bits into ferroelectric memories. This process is allowed by symmetry because a strain gradient, unlike a homogeneous strain, is an odd-parity tensor without inversion symmetry—strain gradients have directionality and polarity (*8*, *9*). Although flexoelectricity is generally weaker than piezoelectricity, gradients grow in inverse proportion to the relaxation length, so very large flexoelectric effects can be achieved at the nanoscale (*10*–*12*).

We have explored whether flexoelectricity can actively switch ferroelectric polarization by mechanically pushing AFM tips onto the surface of epitaxial single-crystalline $BaTiO_3$ films, thereby inducing large and localized stresses. The films were fabricated by atomic layer controlled growth on atomically smooth (001) $SrTiO_3$ substrates with $La_{0.67}Sr_{0.33}MnO_3$ conductive buffers that served as bottom electrodes (*13*, *14*). Compressive stress induced by the substrate ensured that polarization was aligned in the direction perpendicular to the surface, and only 180° inversion of polarization would be allowed. $BaTiO_3$ films with a thickness of 12 unit cells, or ~4.8 nm, have been chosen so as to ensure epitaxial clamping and prevent mismatch strain relaxation (*15*).

Initial testing of the films by means of piezoresponse force microscopy (PFM) show that as-grown $BaTiO_3$ films are in a single-domain state with out-of-plane polarization, indicating effective screening of the depolarizing field by surface adsorbates (*16*). Bipolar domain patterns can be generated conventionally with an electrically biased PFM tip: the film surface is scanned with a tip under ±4-V bias exceeding the coercive voltage. The 2-by-2–μm^2 PFM images of this electrically written domain structure are shown in Fig. 1, A and B. A typical value of the contact force during conventional PFM imaging is ~30 nN. A stable and uniform PFM amplitude signal across the domain boundary illustrates effective electric switchability of the film and strong polarization retention. Local PFM spectroscopic measurements (Fig. 1C) exhibit bipolar piezoelectric hysteresis loops.

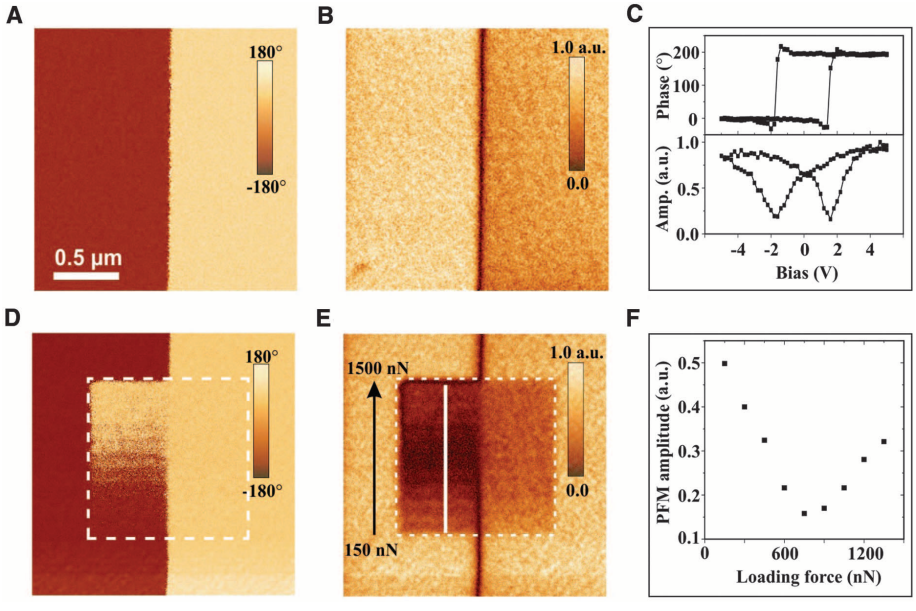

Fig. 1. Mechanically induced reversal of ferroelectric polarization. (**A** and **B**) PFM phase (A) and amplitude (B) images of the bidomain pattern electrically written in the $BaTiO_3$ film. (**C**) Single-point PFM hysteresis loops of the $BaTiO_3$ film. (**D** and **E**) PFM phase (D) and amplitude (E) images of the same area after the 1-by-1–μm^2 area in the center (denoted by a dashed-line frame) has been scanned with the tip under an incrementally increasing loading force. The loading force was increasing in the bottom-up direction [denoted by a black arrow in (E)] from 150 to 1500 nN. (**F**) PFM amplitude as a function of the loading force obtained by cross-section analysis along the white vertical line in (E).

[1]Department of Physics and Astronomy, University of Nebraska–Lincoln, Lincoln, NE 68588, USA. [2]Department of Materials Science and Engineering, University of Wisconsin–Madison, Madison, WI 53706, USA. [3]Department of Fluid Mechanics, Grupo Interdepartamental para la Colaboración Científica Aplicada (GRICCA), Universitat Politecnica de Catalunya, Barcelona, Spain. [4]Department of Materials Science and Metallurgical Engineering, GRICCA, Universitat Politecnica de Catalunya, Barcelona, Spain. [5]Institut Catala de Recerca i Estudis Avançats, (ICREA) Catalunya, Spain. [6]Centre for Investigations in Nanoscience and Nanotechnology (CIN2), Consejo Superior de Investigaciones Cientificas (CSIC) and Institut Catala de Nanotecnologia (ICN), Campus de Bellaterra, Barcelona, Spain.

*To whom correspondence should be addressed. E-mail: gustau.catalan@cin2.es (G.C.); agruverman2@unl.edu (A.G.)

The mechanical switching has been investigated by scanning a 1-by-1–μm^2 area of the bipolar domain pattern with the electrically grounded tip under an incrementally increasing loading force from 150 to 1500 nN, with a corresponding change in the applied stress from 0.5 to 5 GPa (approximating the tip-surface contact area as a disk of 10 nm in radius). Note that, although the maximum local stress is very large, it is still well below the threshold (~20 GPa) for irreversible plastic damage of the $BaTiO_3$ surface (*17*). After that, a larger area of 2 by 2 μm^2 is imaged by conventional PFM with a low load of 30 nN (Fig. 1, D and E).

The tip-induced stress reverses the PFM phase contrast in the left half of the image in Fig. 1D, from dark to bright, indicating inversion of the polarization from up to down. Figure 1E shows a nonmonotonous change in the corresponding PFM amplitude image of the flexoelectrically switched domain: Initially, the amplitude decreases as load increases and then, at an applied force of ~750 nN, it increases again (Fig. 1F). This type of behavior is analogous to the polarization-reversal process in conventional (voltage-induced) PFM (fig. S1) (*18*) in which the electromechanical amplitude signal passes through a minimum during switching, as in Fig. 1C. This is caused by the formation of 180° domains (antiparallel polarization) so that the net polarization and associated piezoelectric signal go through zero when the volume fractions of domains with opposite polarization become equal. Beyond that, the PFM amplitude grows again while the PFM phase is changed by 180°, indicating that the polarization has been inverted. For reference, the PFM images of conventionally (that is, electrically) switched domains in the same $BaTiO_3$ film are shown in the supplementary materials (fig. S1) (*18*). The polarization patterns generated by an electrical bias (fig. S1) (*18*) and by mechanical load (Fig. 1) are identical.

To rationalize the obtained results, we performed finite-element calculations of the strain induced by the AFM tip when pressed against the $BaTiO_3$ film surface (the structure is sketched in Fig. 2A). The calculations are for a tip force of 1000 nN over a tip-sample contact area of 10-nm radius, and the calculated strain distributions for all the strain components are mapped (fig. S2) (*18*). Using the calculated strain gradients, the flexoelectric field is obtained by multiplying the strain gradient times the flexoelectric tensor and dividing by the dielectric constant (*9*, *19*). To be conservative in our calculations, we use the theoretical values for the flexoelectric tensor coefficients (*20*), which are a thousand times smaller than the experimental ones (*21*, *22*). The integral of the flexoelectric field is the flexoelectric potential, which we have calculated and is mapped in Fig. 2B [details of the calculations are provided in (*18*)].

The flexoelectric field was also incorporated into free-energy calculations of the $BaTiO_3$ thin film epitaxially clamped on the $SrTiO_3$ substrate (Fig. 2C). Under a homogeneous compressive uniaxial stress (*23*), the height of the barrier separating the two energy minima is decreased, but the double well remains symmetric, and thus no specific polarity is favored, as expected from symmetry. Flexoelectricity, on the other hand, generates a polar bias consistent with the experimental observation of mechanical switching. When incorporated to the free energy, the flexoelectric bias destabilizes the positive side (upward-pointing polarization) of the double well and forces the switch to the downward-pointing polarization state, as observed. This is supported by PFM hysteresis loops measured during application of mechanical stress: As the tip pressure is increased, the positive coercive bias decreases, whereas the negative coercive bias remains intact (fig. S3) (*18*).

For the loading force of 1000 nN, the calculated flexoelectric field reaches a maximum of 2 MV/cm, comparable with the intrinsic coercive field (theoretical) and that extracted from the piezo-

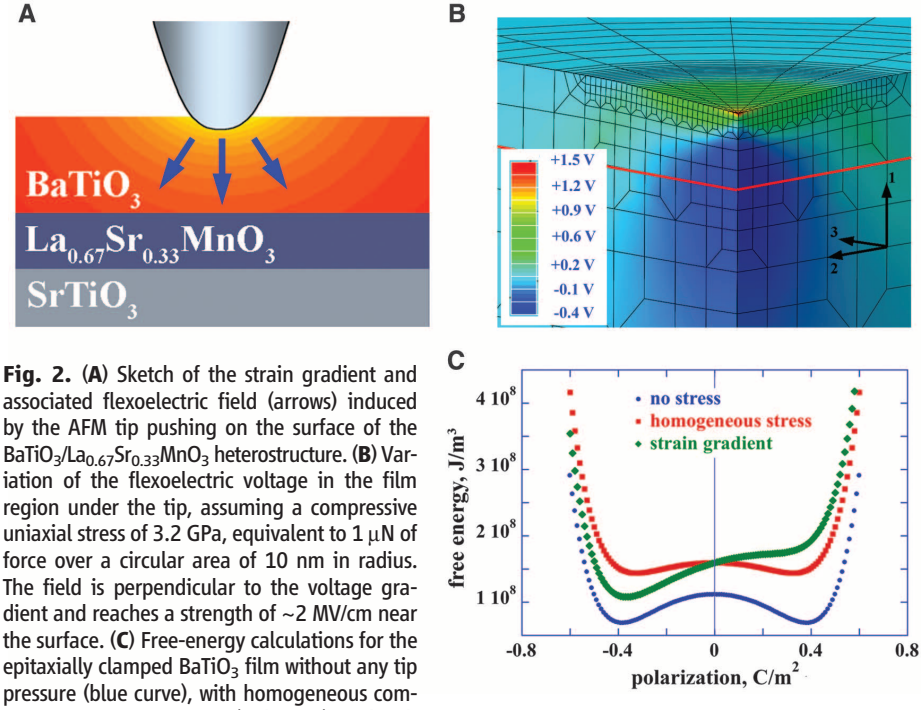

Fig. 2. (**A**) Sketch of the strain gradient and associated flexoelectric field (arrows) induced by the AFM tip pushing on the surface of the $BaTiO_3/La_{0.67}Sr_{0.33}MnO_3$ heterostructure. (**B**) Variation of the flexoelectric voltage in the film region under the tip, assuming a compressive uniaxial stress of 3.2 GPa, equivalent to 1 μN of force over a circular area of 10 nm in radius. The field is perpendicular to the voltage gradient and reaches a strength of ~2 MV/cm near the surface. (**C**) Free-energy calculations for the epitaxially clamped $BaTiO_3$ film without any tip pressure (blue curve), with homogeneous compressive stress of 3.2 GPa (red curve), and with the calculated flexoelectricity from the tip-induced strain gradient (green curve). Flexoelectricity skews the double well, forcing polarization switching toward the stable downward state.

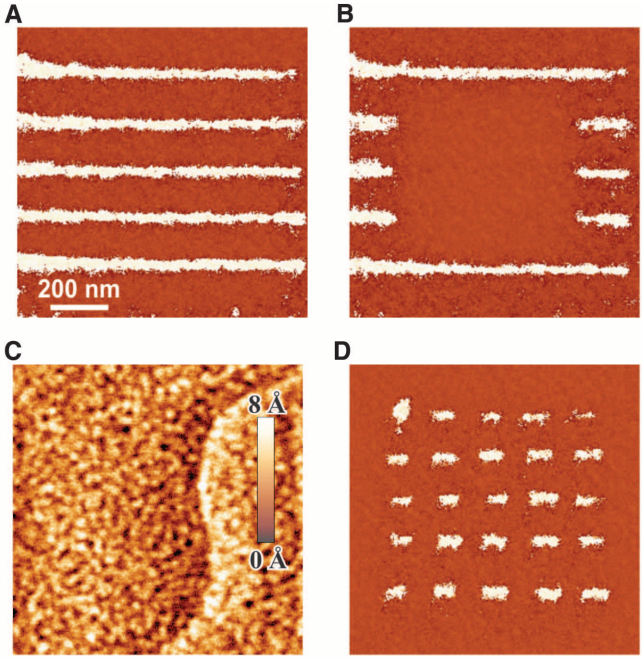

Fig. 3. Fabrication of nanoscale domain patterns by mechanical means. (**A**) Domain lines mechanically written in the $BaTiO_3$ film by scanning the film with a tip under a loading force of 1500 nN. (**B**) The same domain structure modified by electrical erasure of the mechanically written domains. Erasure has been performed by scanning the central segment with the tip under a dc −3-V bias. (**C**) Topographic image of the same area acquired after mechanical writing showing that the film surface was not affected by the writing process. (**D**) An array of flexoelectrically written dot domains illustrating the possibility of using mechanical writing for high-density data-storage application.

electric hysteresis loops (experimental). Note that such a large flexoelectric field has been obtained in spite of our conservative choice of flexoelectric coefficients, supporting the feasibility of the flexoelectric switching mechanism. We stress that the Landau formalism provides an upper limit for the ideal (intrinsic) switching barrier; in practice, there will be defects that act as nucleation sites facilitating the switching at lower coercive fields. In real devices, therefore, the effective coercive field may be considerably lower than calculated here, meaning that the flexoelectric field will be capable of inducing switching at lower loads or larger thicknesses than assumed here.

There are several useful features of mechanical switching: (i) It generates stable domain patterns exhibiting no relaxation for days after switching, (ii) mechanically written domain patterns are electrically erasable, (iii) no damage to the sample surface caused by a high loading force was observed, and (iv) the mechanically written domains are nanoscopic. These features are illustrated in Fig. 3. Mechanically written parallel linear domains, shown in Fig. 3A, have been subsequently transformed into the pattern in Fig. 3B by electrically erasing central domain segments with a tip under a dc –3-V bias. The topographic image of the same area of the $BaTiO_3$ film (Fig. 3C), acquired after this procedure, does not exhibit any traces of surface deformation. Finally, Fig. 3D shows an array of dot domains only 30 nm in size, written by abruptly alternating the tip load between 30 and 1500 nN during scanning.

These results open up a way to write ferroelectric memory bits using mechanical force instead of electrical bias in data-storage devices. By converting mechanical stress into readable information, such devices would operate as a nanoscopic analog of typewriters that could be scaled up using a millipede-like scheme (*24*). The tip-sample contact area is typically less than 10-nm in radius, so switching can be highly localized, allowing fabrication of high-density domain patterns. Because no voltage is applied during mechanical switching, leakage and/or dielectric breakdown problems are minimized [in fact, even insulating tips can be used to mechanically write the domains, as shown in fig. S4 (*18*)]. Because electrodes are not required, the problems caused by their finite screening length (*25*) are also removed.

Conversely, if top electrodes were used, mechanical writing would enable the targeted poling of localized areas under the electrodes—which is impossible using voltage, as the electric field is homogeneous in a parallel-plate capacitor. This suggests the possibility of controlled fabrication of domain walls underneath top electrodes, useful for electronic device applications employing physical properties of domain walls (*26*) that could be read in a nondestructive manner by PFM imaging (*27*) or by measuring the electroresistive effect (*28*).

References and Notes

1. K. J. Choi *et al.*, *Science* **306**, 1005 (2004).
2. G. Catalan *et al.*, *Phys. Rev. Lett.* **96**, 127602 (2006).
3. G. Zavala, J. H. Fendler, S. Trolier-McKinstry, *J. Appl. Phys.* **81**, 7480 (1997).
4. A. Kholkin *et al.*, *Appl. Phys. Lett.* **82**, 2127 (2003).
5. A. Gruverman, A. Kholkin, A. Kingon, H. Tokumoto, *Appl. Phys. Lett.* **78**, 2751 (2001).
6. D. Lee *et al.*, *Phys. Rev. Lett.* **107**, 057602 (2011).
7. A. Gruverman *et al.*, *Appl. Phys. Lett.* **83**, 728 (2003).
8. S. M. Kogan, *Sov. Phys. Solid State* **5**, 2069 (1964).
9. J. F. Scott, *J. Chem. Phys.* **48**, 874 (1968).
10. G. Catalan, L. J. Sinnamon, J. M. Gregg, *J. Phys. Condens. Matter* **16**, 2253 (2004).
11. G. Catalan *et al.*, *Nat. Mater.* **10**, 963 (2011).
12. M. S. Majdoub, P. Sharma, T. Çağin, *Phys. Rev. B* **78**, 121407 (2008).
13. C. B. Eom *et al.*, *Science* **258**, 1766 (1992).
14. L. J. Belenky, X. Ke, M. Rzchowski, C. B. Eom, *J. Appl. Phys.* **97**, 10J107 (2005).
15. In our studies, the flexoelectric switching has been demonstrated in films with thickness of up to 48 unit cells.
16. D. D. Fong *et al.*, *Phys. Rev. Lett.* **96**, 127601 (2006).
17. Y. Gaillard, A. Hurtado Macías, J. Muñoz-Saldaña, M. Anglada, G. Trápaga, *J. Phys. D Appl. Phys.* **42**, 085502 (2009).
18. Supplementary materials are available on *Science* Online.
19. W. Ma, *Phys. Status Solidi B* **245**, 761 (2008).
20. R. Maranganti, P. Sharma, *Phys. Rev. B* **80**, 054109 (2009).
21. W. Ma, L. E. Cross, *Appl. Phys. Lett.* **88**, 232902 (2006).
22. J. Hong, G. Catalan, J. F. Scott, E. Artacho, *J. Phys. Condens. Matter* **22**, 112201 (2010).
23. A. Yu. Emelyanov, N. A. Pertsev, A. L. Kholkin, *Phys. Rev. B* **66**, 214108 (2002).
24. P. Vettiger *et al.*, *IEEE Trans. NanoTechnol.* **1**, 39 (2002).
25. V. Nagarajan *et al.*, *J. Appl. Phys.* **100**, 051609 (2006).
26. G. Catalan, J. Seidel, R. Ramesh, J. F. Scott, *Rev. Mod. Phys.* **84**, 119 (2012).
27. D. A. Bonnell, S. V. Kalinin, A. Kholkin, A. Gruverman, *MRS Bull.* **34**, 648 (2009).
28. V. Garcia *et al.*, *Nature* **460**, 81 (2009).

Acknowledgments: A.G and G.C. conceived the idea, designed the experiment, and wrote the paper; H.L. implemented experimental measurements; C.-W.B. fabricated the samples; C.-B.E. supervised sample preparation and reviewed the paper; and D.E.O., J.A., and G.C. performed finite-element and free-energy calculations. G.C. and A.G. thank the Leverhulme Trust for international network funding (F/00 203/V) for the funds that have enabled this collaboration. G.C. acknowledges financial support from grants MAT2010-10067-E and MAT2010-17771, and J.A. acknowledges support from grant MAT2011-23375 (Ministerio de Educación, Ciencia e Innovación). The work at Univ. of Nebraska-Lincoln was supported by the Materials Research Science and Engineering Center (NSF grant DMR-0820521) and by the U.S. Department of Energy (DOE), Office of Basic Energy Sciences, Division of Materials Sciences and Engineering (DOE grant DE-SC0004876). The work at Univ. of Wisconsin–Madison was supported by the NSF under grant ECCS-0708759.

Supplementary Materials

www.sciencemag.org/cgi/content/full/336/6077/59/DC1
Materials and Methods
Supplementary Text
Figs. S1 to S4
References

4 January 2012; accepted 23 February 2012
10.1126/science.1218693

High-Resolution EM of Colloidal Nanocrystal Growth Using Graphene Liquid Cells

Jong Min Yuk,[1,2,3]* Jungwon Park,[2,4]* Peter Ercius,[5] Kwanpyo Kim,[1,2,6] Daniel J. Hellebusch,[4] Michael F. Crommie,[1,2,6] Jeong Yong Lee,[3]† A. Zettl,[1,2,6]† A. Paul Alivisatos[2,4]†

We introduce a new type of liquid cell for in situ transmission electron microscopy (TEM) based on entrapment of a liquid film between layers of graphene. The graphene liquid cell facilitates atomic-level resolution imaging while sustaining the most realistic liquid conditions achievable under electron-beam radiation. We employ this cell to explore the mechanism of colloidal platinum nanocrystal growth. Direct atomic-resolution imaging allows us to visualize critical steps in the process, including site-selective coalescence, structural reshaping after coalescence, and surface faceting.

A wide range of physical, chemical, and biological phenomena that take place in liquids on the nanometer scale would benefit from observations with atomic resolution transmission electron microscopy (TEM). EM techniques such as conventional TEM (CTEM), scanning TEM (STEM), and four-dimensional (4D) EM have enabled direct observation of solid-phase phenomena with atomic resolution (*1*–*4*). Applying these effective imaging tools to the study of liquid-phase phenomena is hampered by difficulties in maintaining realistic conditions for the liquid specimen (*5*). For example, TEM requires high vacuum conditions, which are generally incompatible with liquid samples. One way to overcome this constraint is to employ environmental cells that contain a sealed reservoir with a viewing window fabricated from Si_3N_4 or SiO_2 (*6*–*8*). Although such liquid cells have enabled studies of nanoscale phenomena, the relatively thick (tens to one hundred nanometers) and relatively high atomic number (Z) element windows have poor electron transmittance, resulting in reduced sensitivity and a resolution limit of a few nanometers. Unfortunately, true atomic-resolution imaging cannot be achieved, and furthermore, the thick cell windows also appear to perturb the natural state of the liquid or species suspended in the liquid.

An example of the benefits that could arise from atomic-resolution imaging in nonperturbative